



# Early effect of $^{90}\text{Y}$ radioembolisation on hepatocellular carcinoma and liver parenchyma stiffness measured with MR elastography: initial experience

Paul Kennedy<sup>1</sup> · Sara Lewis<sup>1,2</sup> · Octavia Bane<sup>1</sup> · Stefanie J Hectors<sup>1,3</sup> · Edward Kim<sup>2</sup> · Myron Schwartz<sup>4</sup> · Bachir Taouli<sup>1,2</sup> 

Received: 21 May 2020 / Revised: 24 November 2020 / Accepted: 16 December 2020 / Published online: 21 January 2021  
© European Society of Radiology 2021

## Abstract

**Objectives** To quantify hepatocellular carcinoma (HCC) and liver parenchyma stiffness using MR elastography (MRE) and serum alpha fetoprotein (AFP), before and 6 weeks (6w) after  $^{90}\text{Y}$  radioembolisation (RE), and to assess the value of baseline tumour and liver stiffness (TS/LS) and AFP in predicting response at 6w and 6 months (6 m).

**Methods** Twenty-three patients (M/F 18/5, mean age  $68.3 \pm 9.3$  years) scheduled to undergo RE were recruited into this prospective single-centre study. Patients underwent an MRI exam at baseline and 6w following RE (range 39–47 days) which included MRE using a prototype 2D EPI sequence. TS, peritumoural LS/LS remote from the tumour, tumour size, and AFP were measured at baseline and at 6w. Treatment response was determined using mRECIST at 6w and 6 m.

**Results** MRE was technically successful in 17 tumours which were classified at 6w as complete response (CR,  $n = 7$ ), partial response (PR,  $n = 4$ ), and stable disease (SD,  $n = 6$ ). TS and peritumoural LS were significantly increased following RE ( $p = 0.016$ ,  $p = 0.039$ , respectively), while LS remote from tumour was unchanged ( $p = 0.245$ ). Baseline TS was significantly lower in patients who achieved CR at 6w ( $p = 0.014$ ). Baseline TS, peritumoural LS (both AUC = 0.857), and AFP (AUC = 0.798) showed fair/excellent diagnostic performance in predicting CR at 6w, but were not significant predictors of OR or CR at 6 m.

**Conclusion** Our initial results suggest that HCC TS and peritumoural LS increase early after RE. Baseline TS, peritumoural LS, and AFP were all significant predictors of CR to RE at 6w. These results should be confirmed in a larger study.

## Key Points

- *Magnetic resonance elastography–derived tumour stiffness and peritumoural liver stiffness increase significantly at 6 weeks post radioembolisation whereas liver stiffness remote from the tumour is unchanged.*
- *Baseline tumour stiffness and peritumoural liver stiffness are lower in patients who achieve complete response at 6 weeks post radioembolisation.*
- *Baseline tumour size is significantly correlated with baseline tumour stiffness.*

**Keywords** Elasticity imaging techniques · Carcinoma, hepatocellular · Yttrium-90

✉ Bachir Taouli  
bachir.taouli@mountsinai.org

<sup>1</sup> BioMedical Engineering and Imaging Institute, Icahn School of Medicine at Mount Sinai, New York, NY, USA

<sup>2</sup> Department of Diagnostic, Molecular and Interventional Radiology, Icahn School of Medicine at Mount Sinai, 1470 Madison Avenue, New York, NY 10029, USA

<sup>3</sup> Department of Radiology, Weill Cornell Medicine, New York, NY, USA

<sup>4</sup> Recanati/Miller Transplantation Institute, Icahn School of Medicine at Mount Sinai, New York, NY, USA

## Abbreviations

AFP	Alpha fetoprotein
LS	Liver stiffness
MRE	Magnetic resonance elastography
RE	$^{90}\text{Y}$ radioembolisation
TS	Tumour stiffness
VOI	Volume of interest

## Introduction

Hepatocellular carcinoma (HCC) is the most prevalent primary liver cancer and is treated with liver transplant or resection

in the early stages. However, in cases of advanced HCC, these options are often not possible. Locoregional therapy such as Yttrium 90 ( $^{90}\text{Y}$ ) radioembolisation (RE) has been used to successfully downstage HCC tumours for local tumour control or to serve as a bridge to liver transplantation [1]. At our institution, early-stage patients planned for liver transplantation also undergo locoregional therapy while waiting. During RE,  $^{90}\text{Y}$  glass microspheres are administered through intra-arterial hepatic infusion in a segmental or lobar fashion. The diameter of the glass microspheres is too large to pass to venous circulation and they become trapped in the tumour capillary bed, delivering a high radiation dose to the arterially perfused tumour while sparing the predominantly portal-venously perfused liver parenchyma [2].

Previous reports have highlighted radiological findings following RE [3]. The standard criteria for HCC response are the modified response evaluation criteria in solid tumours (mRECIST) and more recently LI-RADS response criteria, which rely upon contrast-enhanced CT or MRI [4–6]. At our institution, patients who have received RE routinely undergo imaging at 6 weeks (6w) to assess technical efficiency and early tumour response. Non-invasive quantitative imaging techniques which can predict tumour response would be of great clinical benefit by informing clinicians on the likelihood of positive therapy outcomes. This could lead to changes in clinical management e.g. only performing therapies with likelihood of success rather than high risk, expensive treatments with very low chance of patient benefit. Diffusion-weighted imaging (DWI) is one technique which has shown promise as a predictor of tumour response post-RE [7, 8]. In addition to changes in cellularity, radiation effects include perivascular oedema, inflammation, extracellular matrix remodelling, and peritumoural liver fibrosis [9, 10]. These changes are likely to influence the mechanical microenvironment and may be measurable as a change in tissue stiffness. Tumour stiffness is determined by factors such as interstitial pressure and extracellular matrix reorganisation. These factors may impact the efficacy of RE and predict the degree of necrosis achieved following RE. MR elastography (MRE) enables the quantification of tissue stiffness and has become a widely used tool for staging liver fibrosis [11–14]. Several studies have assessed liver lesions using MRE and found it useful for lesion characterisation [15–17], differentiating HCC tumour grades [18], and predicting HCC recurrence [19]. There are limited reports on the use of MRE in HCC after locoregional therapy [20] and immunotherapy [21]. The cross-sectional study by Gordic et al [20] reported lower tumour stiffness (TS) in treated vs untreated HCCs (in different groups of patients), while a prospective, longitudinal study of HCC response to immunotherapy reported no significant difference in tumour stiffness at 6w following immunotherapy [21]. There is currently a lack of

longitudinal studies investigating the change in stiffness of HCC tumours and surrounding liver parenchyma following RE.

The aim of our initial study was to quantify early changes in HCC and liver parenchyma stiffness using MRE and serum AFP, before and 6w after RE, and to assess the value of baseline tumour and liver stiffness (TS/LS) and AFP in predicting treatment response at 6w and 6 months (6 m).

## Methods

### Patients

This single-centre prospective study was compliant with the Health Insurance Portability and Accountability Act and approved by the local institutional review board. Between July 2016 and December 2017, a signed informed consent was obtained from 23 treatment-naïve patients (M/F 18/5, mean age  $68.3 \pm 9.3$  years, range 55–93 years) with radiologically diagnosed HCC who were scheduled to undergo clinically indicated RE. Of the 23 patients, 3 declined to undergo repeat research imaging at 6w so only baseline data were available. The mean duration between baseline MRI and RE was  $37 \pm 25$  days (range 3–117 days), with follow-up MRI occurring  $42 \pm 2$  days (range 39–47 days) after RE. Patient clinical and demographic information is shown in Table 1. The patient recruitment flow chart is shown in Fig. 1.

### RE treatment

Prior to RE, all patients underwent a mapping procedure with Tc-99m macroaggregated albumin (MAA). Utilising Tc-99m MAA as a surrogate for  $^{90}\text{Y}$  microspheres enables approximate mapping of hepatic vasculature, highlighting any arterial shunting which could cause unintended radiation dose to other areas in the body. Mapping occurred  $17 \pm 8$  days (range 8–39 days) before RE. During RE, a microcatheter was inserted into the hepatic artery and advanced to the level of the lobar artery ( $n = 4$ ) or further into segmental arterial branches ( $n = 19$ ).  $^{90}\text{Y}$  glass microspheres (TheraSphere, Boston Scientific) were delivered through the catheter and travelled through the arterial vasculature until they were trapped in the feeding arterioles of the tumour, delivering a concentrated radiation dose. The average administered dose was  $1.74 \pm 0.91$  GBq (range 0.80–3.77 GBq).

### MRI acquisition

Baseline and follow-up imaging exams were performed on a 1.5-T MRI system (Aera, Siemens Healthineers) using an 18-channel flexible body array coil and an integrated 32-channel spine coil. Patients were instructed to fast for 4 h prior to

**Table 1** Patient demographics and clinical characteristics

Parameter	Classification	Value
Demographics		
Age (years)	Mean $\pm$ SD (range)	68 $\pm$ 9 (55–93)
Sex	M/F	16/4
Aetiology of liver disease	HCV/NASH/alcohol/HBV/cryptogenic	13/4/1/1/1
Child-Pugh classification	A/B/C	11/9/0
MELD score	Mean $\pm$ SD (range)	11.3 $\pm$ 4.1 (7–24)
BCLC stage	0/A/B/C	2/12/3/3
Multifocal HCC	Yes/no	4/16
Baseline AFP (ng/ml)	Mean $\pm$ SD (range)	749 $\pm$ 2,323 (2.6–10,053)
Baseline tumour size (cm)	Mean $\pm$ SD (range)	3.6 $\pm$ 1.7 (1.5–6.3)
Baseline MRI to RE interval (days)	Mean $\pm$ SD (range)	37 $\pm$ 25 (3–117)
RE to 6m follow-up interval (days)	Mean $\pm$ SD (range)	181 $\pm$ 27 (136–215)

AFP, alpha fetoprotein; BCLC, Barcelona Clinical Liver Cancer classification; HBV, hepatitis B virus; HCV, hepatitis C virus; MELD, model for end-stage liver disease; NASH, nonalcoholic steatohepatitis

imaging. The 2D MRE data in this study were acquired using a work-in-progress (WIP) prototype single-shot spin-echo echo-planar imaging (SE-EPI) sequence. A trapezoidal motion-encoding gradient (MEG) is inserted between the excitation and refocusing pulse which encodes motion in the slice-select direction into the MR phase signal. The frequency of the MEG was matched to the vibration frequency (60 Hz). The onset of the MEG is shifted in fixed increments, equal to the period of external vibration divided by the number of phase offsets acquired (4), relative to the external vibration. Thus, the shear wave propagation is evenly sampled over a vibration period. A 19-cm plastic paddle was placed lateral to the xiphoid process over the upper-right thorax and connected to an active pneumatic driver located outside the scan room. Sixty-hertz vibrations were applied throughout the data acquisition. Ten axial slices were acquired centred over the index lesion. Imaging parameters were repetition time 1500 ms, time to echo 48 ms, matrix size 128  $\times$  128, field of view 360–400 mm<sup>2</sup>, slice thickness 3 mm, iPAT factor 2, and bandwidth 1502 Hz/px. Four offsets of the wave propagation were

obtained in the through-plane direction in acquisition time of 15 s. Acquired 2D MRE data were reconstructed inline using a commercially available 2D multi-model direct inversion (MMDI) algorithm [22]. The algorithm produced magnitude, phase, colourised wave propagation, and elastogram images. A confidence mask was also produced which, when overlaid on the elastogram, highlighted regions of reliable measurement.

In addition to MRE, the multiparametric MRI protocol included axial and coronal T<sub>2</sub>-weighted turbo-spin-echo (HASTE), axial in- and out-of-phase, T<sub>2</sub>\*/T<sub>1</sub> mapping, and DWI. 3D T<sub>1</sub>-VIBE was acquired pre- and 1, 10, and 20 min post-injection of gadoxetic acid (0.025 mmol/kg, Eovist/Primovist). Dynamic contrast-enhanced (DCE)-MRI was also acquired during and after contrast administration. DWI and DCE-MRI data are reported elsewhere [23].

### MRE image analysis

All HCC lesions on baseline and follow-up exams were identified by an abdominal radiologist (SL, observer 1) with 8 years' experience in body MRI. An MR physicist (PK, observer 2) with 4 years of experience drew regions of interest (ROIs) in index lesions, peritumoural liver parenchyma (1.5-cm donut-shaped ROI around the lesion where possible, avoiding vessels and staying 1 cm away from the liver capsule) and in liver parenchyma remote to the treated liver segment/lobe on the MRE magnitude images using the ImageJ software (NIH) [23]. MRE ROI location was confirmed to be appropriate by observer 1. Stiffness was measured for each ROI in all captured slices with a mean value recorded, weighted by ROI size. Care was taken to include only regions within the 95% confidence map with visible wave propagation. If more than 2 lesions were identified, the largest lesion receiving RE was chosen. Necrotic tumour

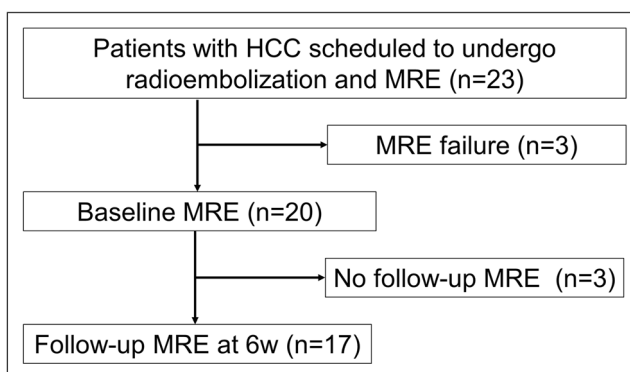


**Fig. 1** Flow diagram showing patient recruitment for the study

regions were included in the ROIs both at baseline and follow-up. Percentage stiffness change was calculated as: [(post-RE stiffness - baseline stiffness)/baseline stiffness × 100%] for tumour (TS) and liver parenchyma (LS) peritumourally and remote to the tumour.

### Assessment of tumour response

Tumour size at baseline and 6w was measured on pre-/post-contrast 3D T<sub>1</sub>-weighted images by observer 1, with the longest diameter of viable tumour recorded. Treatment response was assessed on imaging obtained at 6w and 6m following RE by observer 1. Tumour response was based on modified response evaluation criteria in solid tumours (mRECIST) using the following classifications: complete response (CR): no intratumoural arterial enhancement; partial response (PR): ≥ 30% decrease in the sum of the diameters of viable (arterially enhancing) target lesions; stable disease (SD): any case that does not qualify for either PR or progressing disease and; progressive disease (PD): ≥ 20% increase in the sum of the diameters of viable (arterially enhancing) target lesions. Patients who achieved CR or PR were classified as having an objective response (OR). The degree of tumour necrosis was determined from subtracted post-contrast 3D T<sub>1</sub>-weighted images by observer 1 [5]. The presence of haemorrhage following RE was also assessed by observer 1 based on qualitative assessment of pre-contrast T<sub>1</sub>-weighted images (as present/absent T<sub>1</sub> hyperintense signal in the tumour). Arterial enhancement was assessed at 25–35 s post-contrast administration on DCE-MR images.

### Statistical analysis

Pre- and post-RE TS and peritumoural/remote LS were compared using Wilcoxon signed-rank tests. A Kruskal-Wallis test was used to compare TS and peritumoural/remote LS at baseline. Mann-Whitney *U* tests were used to compare TS, peritumoural/remote LS, tumour size, and AFP (all at baseline) based on OR vs SD and CR vs PR/SD. The difference in TS at 6w in tumours with/without haemorrhage was also assessed using Mann-Whitney *U* tests. Spearman correlation analysis was used to determine the relationships between baseline TS and tumour size, post-treatment TS, and degree of necrosis at 6w as well as tumour size at 6w. ROC analysis was used to determine the ability of TS and peritumoural/remote LS, changes in TS and LS, tumour size, and AFP to predict response at 6w and 6m. The DeLong test was used to determine differences between AUC values. Stepwise binary logistic regression was used to identify significant combinations of MRE measures, tumour size, and AFP for prediction of response. Statistical analysis was performed using SPSS (v20, IBM Corporation). The DeLong test was performed

using MedCalc (v19.2, MedCalc Software). A *p* value < 0.05 was considered significant.

## Results

### Technical success of MRE

MRE was technically successful in 20/23 (87%) patients. MRE failed in 3/23 (13%) patients due to massive ascites (*n* = 2) and interposed colon attenuating shear waves (*n* = 1). In the 20 patients with MRE at baseline, MRE data were available in tumours (*n* = 17), peritumoural liver parenchyma (*n* = 16), and liver parenchyma remote from tumour (*n* = 18). Three patients declined research follow at 6w. Six-week follow-up MRE data were available in tumours (*n* = 14), peritumoural liver parenchyma (*n* = 13), and liver parenchyma remote from tumour (*n* = 14). Factors affecting data availability were the location of MRE imaging plane, deep-lying tumours causing wave attenuation and hence poor stiffness confidence, and large tumour in the dome of liver allowing only TS measurement. Thus, pre- and post-RE MRE data were available for tumours in 14 patients, peritumoural liver parenchyma in 13 patients, and liver parenchyma remote from the tumour in 14 patients.

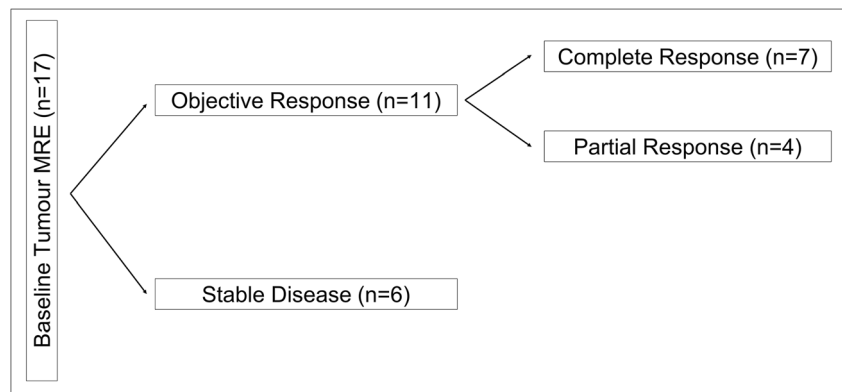
### Tumour response

The mean tumour size at baseline was 3.6 ± 1.7 cm (range 1.5–6.3 cm). Among the patients with successful baseline TS measurements, 11/17 (65%) achieved OR (CR (*n* = 7), PR (*n* = 4)) at 6w (Fig. 2). Six patients were classified as having SD (2 had retreatment with RE, 1 had retreatment with chemoembolisation, 2 were not subsequently imaged at our institution again, and 1 was deceased before further follow-up). One patient classified as PR was lost to follow-up at 6m. Therefore, 6m follow-up clinical imaging was performed on 10/17 patients with baseline TS measures who did not undergo interval treatment, all of which achieved OR (CR (*n* = 7), PR (*n* = 3)).

### Baseline stiffness

Example pre- and post-RE images are shown in Fig. 3. At baseline, mean LS remote to the tumour and in peritumoural region were not significantly different from TS (5.4 ± 2.1 vs 4.5 ± 1.3 vs 5.4 ± 2.6 kPa, respectively, *p* = 0.562). The mean baseline ROI size per slice was 16.1 ± 9.5 cm<sup>2</sup> (range 35.7–6.8 cm<sup>2</sup>) for LS remote to the tumour, 4.8 ± 2.5 cm<sup>2</sup> (range 9.3–2.2 cm<sup>2</sup>) for peritumoural LS and 4.2 ± 2.6 cm<sup>2</sup> (range 9.6–1.4 cm<sup>2</sup>) for tumour. Combining over all slices in which the target region was included, the mean baseline volume of interest

**Fig. 2** Diagram illustrating tumour response in patients with baseline tumour stiffness measurements



(VOI) size was  $65.8 \pm 44.0 \text{ cm}^3$  (range  $160.7\text{--}19.6 \text{ cm}^2$ ) for LS remote to the tumour,  $11.5 \pm 8.1 \text{ cm}^3$  (range  $31.2\text{--}4.1 \text{ cm}^3$ ) for peritumoural LS, and  $12.2 \pm 9.8 \text{ cm}^3$  (range  $31.6\text{--}2.4 \text{ cm}^2$ ) for tumour. Baseline TS was found to significantly correlate with baseline tumour size ( $r = 0.746, p = 0.001$ ; Fig. 4), while there was no significant correlation between post-RE tumour size and TS post-RE ( $r = 0.179, p = 0.541$ ; Fig. 4).

**Effect of RE on TS and LS**

Baseline and post-RE measurements are displayed in Table 2. TS was found to significantly increase at 6w post-RE ( $p =$

$0.016$ ; Fig. 5) by an average of  $49.3 \pm 62.8\%$ . Specifically, TS increased in 12/14 ( $61.7 \pm 58.9\%$ ) and decreased in 2 tumours ( $- 25.4 \pm 2.9\%$ ). Peritumoural LS was also found to significantly increase following treatment ( $p = 0.039$ ; Fig. 5) by an average of  $38.3 \pm 62.5\%$ . Specifically, peritumoural LS increased in 10/13 patients ( $56.7 \pm 59.3\%$ ) and decreased in 3 patients ( $- 22.6 \pm 19.1\%$ ). LS remote from the tumour did not significantly change following RE ( $- 2.9 \pm 17.4\%, p = 0.245$ ; Fig. 5). Post-RE TS did not correlate with the degree of tumour necrosis at 6w ( $r = - 0.242, p = 0.444$ ). At 6w, 10/14 tumours were classified as haemorrhagic (based on native T1 signal). Post-RE TS was not significantly different in tumours

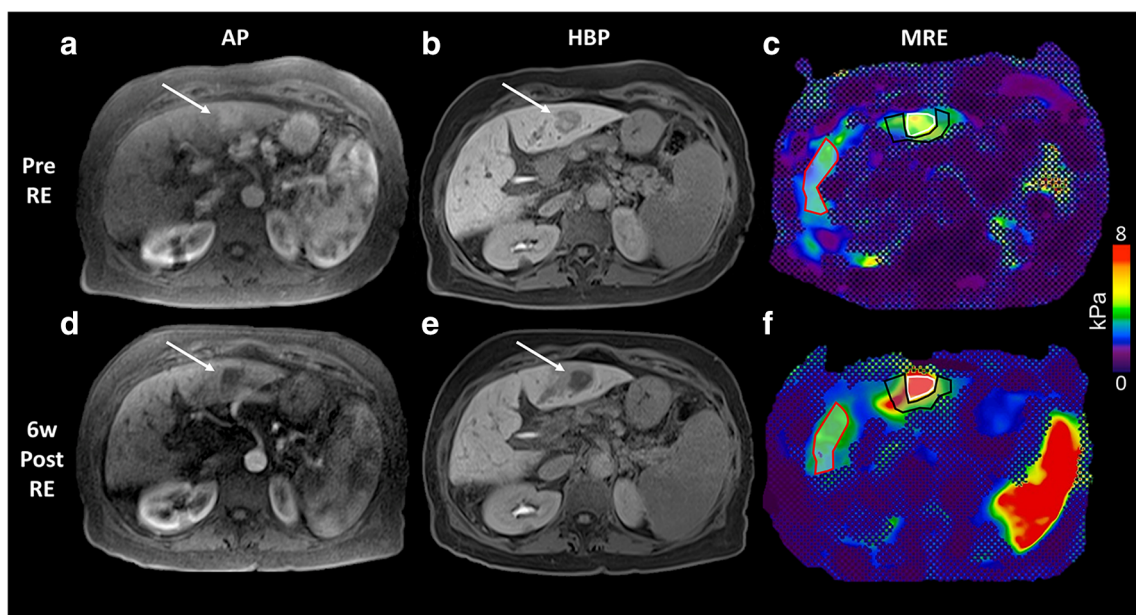


**Fig. 3** MRI and MRE images from a 76-year-old female patient with cryptogenic cirrhosis and HCC pre- (top) and 6 weeks post radioembolization (RE, bottom). Top: Contrast-enhanced T1-weighted images post gadoxetate injection demonstrate arterial phase hyperenhancement (arrow) (a) and hypointensity (b) on hepatobiliary phase, with areas of increased signal (compatible with haemorrhage). c Stiffness map obtained with 2D-EPI MRE sequence illustrates ROIs for tumour (white outline), peritumoural liver tissue (black outline), and remote liver tissue (red outline). Calculated tumour stiffness was  $4.1 \pm 0.8 \text{ kPa}$ , with peritumoural LS of  $2.3 \pm 0.6 \text{ kPa}$  and LS remote from the

tumour of  $2.7 \pm 0.4 \text{ kPa}$ . Bottom: Contrast-enhanced T1-weighted images post gadoxetate injection demonstrate no arterial phase hyperenhancement (arrow) (d) and peritumoural decreased uptake (e) on hepatobiliary phase image. f Stiffness map obtained with 2D-EPI MRE sequence shows increased tumour stiffness at  $8.0 \pm 1.3 \text{ kPa}$ . Similarly, peritumoural liver stiffness increased to  $6.7 \pm 1.4 \text{ kPa}$ , while liver stiffness away from tumour (red outline) was grossly unchanged ( $2.3 \pm 0.4 \text{ kPa}$ ). 6w scan included spleen MRE hence the apparent elevated spleen stiffness

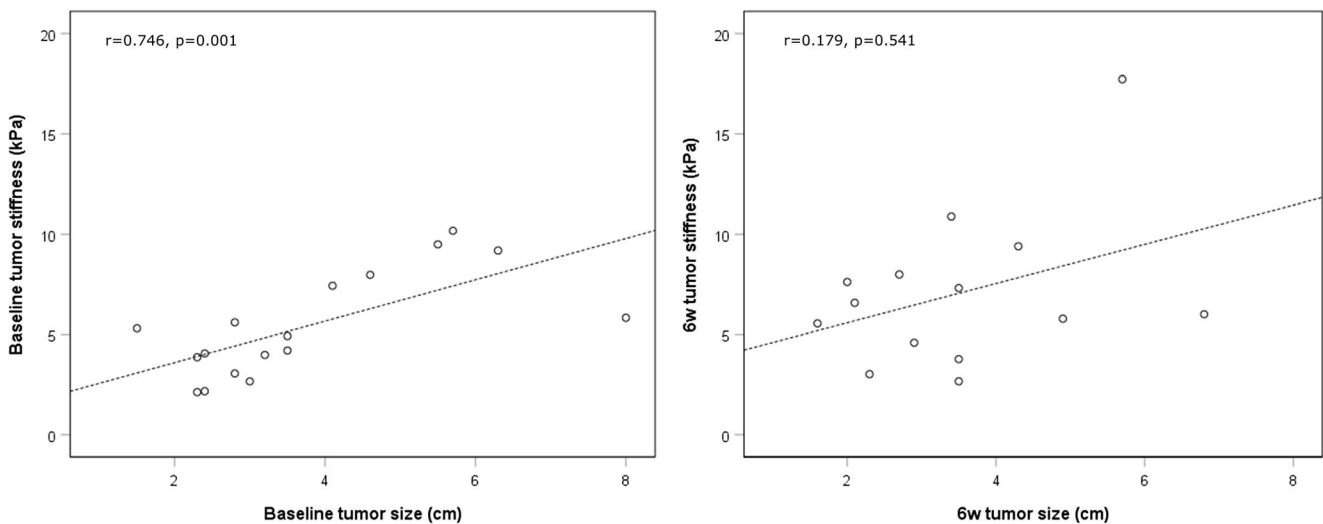


**Fig. 4** Scatter plot illustrating the significant relationship between baseline tumour stiffness and tumour size (left). No correlation was found between tumour stiffness and tumour size following RE (right)

with haemorrhage compared to those without ( $p = 0.242$ ). Mean 6w ROI size per slice was  $15.8 \pm 5.8 \text{ cm}^2$  (range  $24.5\text{--}5.6 \text{ cm}^2$ ) for LS remote to the tumour,  $4.3 \pm 2.9 \text{ cm}^2$  (range  $10.5\text{--}2.0 \text{ cm}^2$ ) for peritumoural LS and  $2.9 \pm 1.7 \text{ cm}^2$  (range  $7.1\text{--}1.4 \text{ cm}^2$ ) for tumours. Combining overall slices in which the target region was included, the mean baseline VOI size was  $65.8 \pm 44.0 \text{ cm}^3$  (range  $160.7\text{--}19.6 \text{ cm}^3$ ) for LS remote to the tumour,  $11.5 \pm 8.1 \text{ cm}^3$  (range  $31.2\text{--}4.1 \text{ cm}^3$ ) for peritumoural LS, and  $12.2 \pm 9.8 \text{ cm}^3$  (range  $31.6\text{--}2.4 \text{ cm}^3$ ) for tumours. There was no significant difference between pre- and post-treatment ROI and VOI size for LS remote to the tumour ( $p = 0.075$  for both), peritumoural LS ( $p = 0.155$  and  $p = 0.477$  respectively), and TS ( $p = 0.064$  for both).

### Prediction of response at 6w and 6m

Patients who achieved CR at 6w had significantly lower baseline TS ( $p = 0.014$ ) and peritumoural LS ( $p = 0.016$ ) compared to patients classified as PR/SD (Table 2; Fig. 6). Although baseline TS in patients who achieved CR at 6m was lower than in those who did not, the difference was not statistically significant ( $p = 0.067$ ). There was no significant difference in TS, LS, peritumoural LS, or the change in TS, LS, and peritumoural LS post-RE in patients who achieved OR vs those classified as SD ( $p > 0.122$ , Table 2). Baseline serum AFP was significantly lower in patients who achieved OR ( $p = 0.041$ ) and CR ( $p = 0.025$ ) at 6w compared to those who did not. There was no significant difference in serum AFP between patients who achieved CR at 6m vs those who did not ( $p = 0.217$ ). Baseline tumour size was not significantly different in patients who achieved OR at 6w ( $p = 0.633$ ) and CR at 6w ( $p = 0.193$ ) or 6m ( $p = 0.067$ ).

The results from ROC analyses are displayed in Table 3. ROC analysis showed that baseline TS and baseline

peritumoural LS were both significant predictors of CR at 6w (AUC 0.857,  $p = 0.015$ , AUC 0.857,  $p = 0.017$ , respectively), although these factors proved not to be significant predictors of OR at 6w or CR at 6m. LS remote from the tumour was not predictive of response at 6w or 6m. Changes in TS and peritumoural/remote LS were not associated with OR at 6w and CR at 6w or 6m (AUC 0.432–0.572,  $p = 0.232\text{--}0.838$ ). Baseline tumour size was not significantly associated with response (AUC 0.577–0.630,  $p = 0.526\text{--}0.710$ ). Baseline serum AFP was a significant predictor of OR (AUC 0.798,  $p = 0.039$ ) and CR (AUC 0.798,  $p = 0.025$ ) at 6w but was not a significant predictor of response at 6m. DeLong tests found no significant differences between the diagnostic performance of MRE parameters and AFP in predicting CR at 6w ( $p = 0.76\text{--}0.91$ ). Logistic regression identified no significant combinations of baseline measures of TS/LS, tumour size, or AFP for prediction of OR or CR at 6w or 6m.

### Discussion

In this study, we assessed the changes in HCC and liver parenchyma stiffness before and after RE in patients with well-compensated liver disease. We found that TS and peritumoural LS significantly increased following RE, while LS remote from the tumour did not change following treatment. A significant correlation between baseline tumour size and TS was observed. Baseline TS and peritumoural LS as well as serum AFP were significant predictors of CR at 6w (patients who achieved CR at 6w were found to have significantly lower baseline TS and peritumoural LS and lower AFP than those who did not).

There are no prior published reports of longitudinal stiffness changes in HCC following RE. A recent study reported

**Table 2** Baseline and 6w MRE stiffness values measured in tumours (TS) and liver parenchyma (LS) in peritumour region and remote from tumour, serum alpha fetoprotein (AFP), and tumour size, in cases classified as complete response (CR), partial response (PR), and stable disease (SD) at 6w. Objective response (OR) includes both CR and PR cases

	All patients	OR	CR	PR	SD	<i>p</i> (OR vs SD) <sup>c</sup>	<i>p</i> (CR vs PR/SD) <sup>c</sup>
Baseline TS (kPa)	5.0 ± 2.5	4.8 ± 2.8	3.5 ± 0.9	6.8 ± 3.7	6.7 ± 2.0	0.122	<i>0.014</i>
6w TS (kPa)	7.0 ± 3.8	6.8 ± 4.4	4.8 ± 2.2	9.8 ± 5.5	7.6 ± 2.4	0.454	0.059
Mean delta (%) <sup>a</sup>	49.3 ± 62.8	48.9 ± 53.4	39.9 ± 44.9	62.3 ± 29.3	50.1 ± 92.1	0.839	> 0.9
<i>p</i> (baseline vs 6w) <sup>b</sup>	<i>0.016</i>	<i>0.022</i>	0.116	0.068	0.273	-	-
Baseline peritumoural LS (kPa)	4.4 ± 1.4	4.2 ± 1.6	3.5 ± 1.2	5.6 ± 1.2	5.0 ± 0.5	0.377	<i>0.016</i>
6w peritumoural LS (kPa)	5.7 ± 2.0	5.2 ± 2.0	4.3 ± 1.4	6.6 ± 2.3	7.3 ± 1.2	0.217	0.051
Mean delta (%) <sup>a</sup>	38.3 ± 62.5	34.9 ± 69.2	47.3 ± 89.1	16.4 ± 18.9	49.6 ± 40.8	0.469	0.945
<i>p</i> (baseline vs 6w) <sup>b</sup>	<i>0.039</i>	0.169	0.345	0.144	0.109	-	-
Baseline LS remote from tumour (kPa)	5.4 ± 2.2	5.3 ± 2.5	5.7 ± 3.0	4.8 ± 1.1	5.9 ± 1.0	0.277	0.258
6w LS remote from tumour (kPa)	5.0 ± 1.4	4.9 ± 1.5	4.9 ± 1.8	5.0 ± 1.1	5.2 ± 0.7	0.659	0.710
Mean delta (%) <sup>a</sup>	-2.9 ± 17.4	-2.1 ± 19.8	-6.1 ± 20.3	4.9 ± 19.2	-6.3 ± 1.5	0.937	0.731
<i>p</i> (baseline vs 6w) <sup>b</sup>	0.245	0.374	0.176	0.715	0.109	-	-
Baseline AFP (ng/ml)	749 ± 2323	277 ± 927	36 ± 73	711 ± 1554	1850 ± 4025	<i>0.041</i>	<i>0.025</i>
6w AFP (ng/ml)	230 ± 735	10 ± 7	13 ± 6	4 ± 3	744 ± 1266	<i>0.002</i>	0.941
Mean delta (%) <sup>a</sup>	38.7 ± 176	51.5 ± 209.7	117.2 ± 238.3	-61.1 ± 41.1	-8.8 ± 53.0	0.494	0.152
<i>p</i> (baseline vs 6w) <sup>b</sup>	0.550	0.331	0.859	0.080	0.917	-	-
Baseline tumour size (cm)	3.46 ± 1.76	3.08 ± 1.39	2.66 ± 0.77	3.84 ± 2.00	4.33 ± 2.32	0.312	0.201
6w tumour size (cm)	3.50 ± 1.66	3.07 ± 1.38	2.64 ± 0.91	3.76 ± 1.82	4.62 ± 1.94	0.173	0.101
Mean delta (%) <sup>a</sup>	8.5 ± 45.3	5.5 ± 51.6	0.8 ± 28.4	13.0 ± 80.5	16.3 ± 24.5	0.246	0.965
<i>p</i> (baseline vs 6w) <sup>b</sup>	0.975	0.678	0.500	0.715	0.498	-	-

<sup>a</sup> Calculated as (post-treatment stiffness-baseline stiffness)/baseline stiffness × 100%

<sup>b</sup> Wilcoxon signed-rank test

<sup>c</sup> Mann-Whitney *U* test

Italicised *p* values denote significance

no significant change in HCC TS at 6w following immunotherapy [21]. The authors did note a significant positive correlation between change in TS following therapy and both overall survival and time to recurrence. We did not assess

overall survival and time to recurrence in our study; however, we did not find that change in TS following therapy was a predictor of response at 6w or 6m. This may be due to the differing mechanisms of action between immunotherapy and

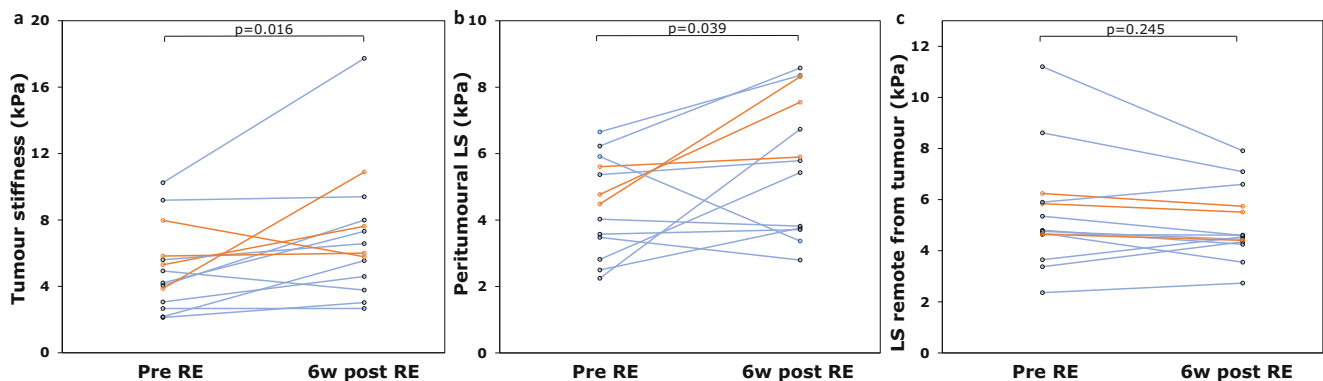


**Fig. 5** Linked plots showing changes in stiffness of tumour (left), peritumoural liver parenchyma (middle), and remote liver parenchyma (right) following radioembolization. Patients with tumours classified as objective response (including complete and partial response) at 6w are highlighted in blue and those classified as stable disease are highlighted in

orange. TS was increased by an average of 49.3% (12/14 increased), peritumoural LS was increased by an average of 38.3% (10/13 increased), and LS remote to the tumour was reduced by an average of 2.9% (10/14 reduced)

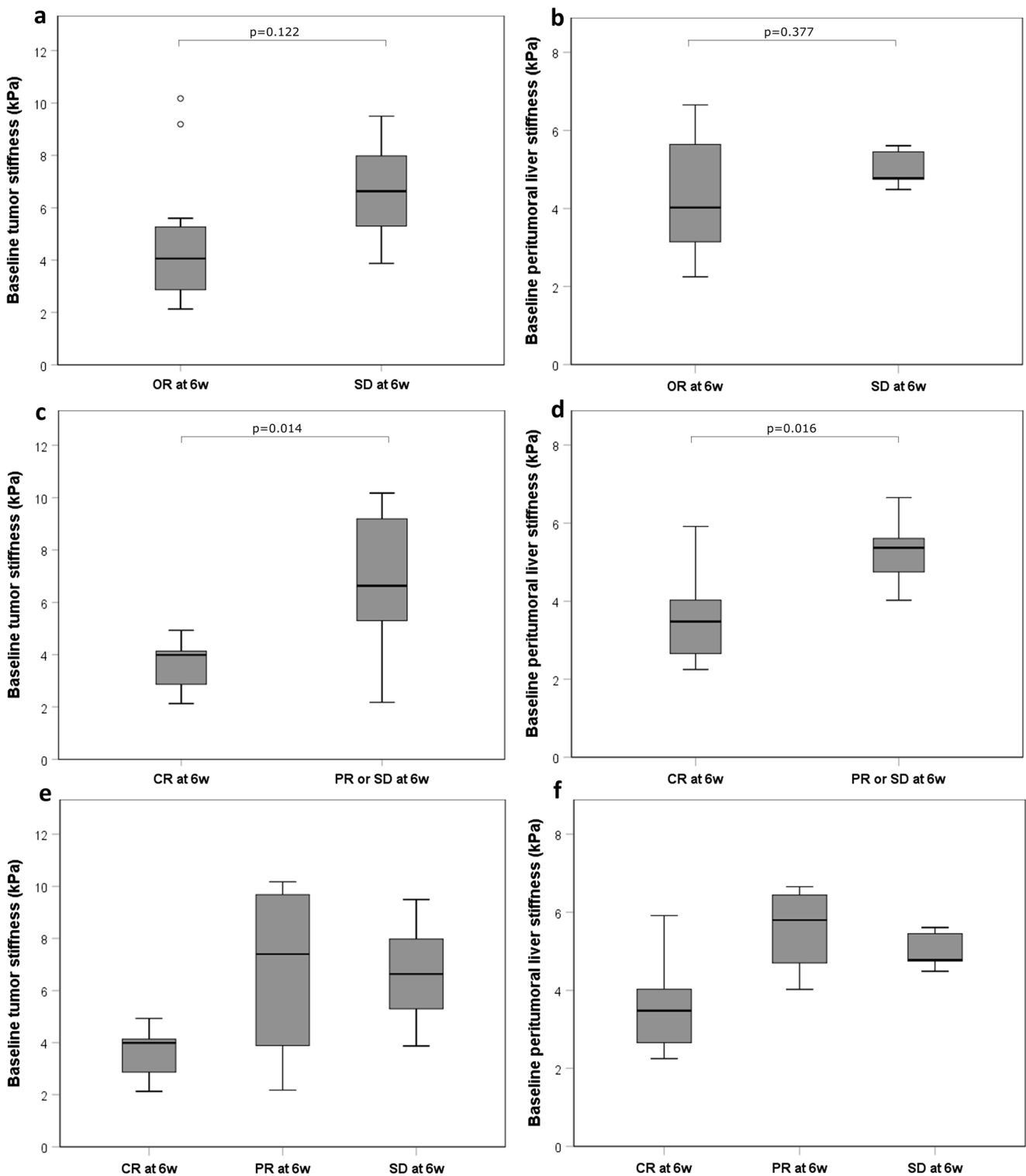


**Fig. 6** Box plots illustrating the difference in baseline tumour stiffness in patients who achieved OR vs SD (a), patients who achieved CR vs PR and SD (c), and patients in all three response groups (e). Peritumoral liver stiffness in patients who achieved OR vs SD (b), patients who

achieved CR vs PR and SD (d), and patients in all three response groups (f) is also shown. CR, complete response; PR, partial response; SD, stable disease; OR, objective response (CR + PR)

RE. A recent study assessed TS in colorectal liver metastases after chemoembolisation and found a significant increase in TS at 6w following therapy, similar to our study [24]. These

results indicate that chemoembolisation and RE both produce an early increase in TS in liver tumours following treatment. It has been previously suggested from in vitro atomic force



**Table 3** Area under the curves (AUC), 95 % confidence intervals (CI), and *p* values for baseline tumour stiffness (TS) and liver stiffness (LS) peritumourally and remote from tumour, serum alpha fetoprotein (AFP),

and tumour size in predicting tumour response at 6w and 6m based on the mRECIST criteria. All patients achieved OR at 6m; hence, AUC analyses were not performed for this response parameter

	Prediction of OR at 6w			Prediction of CR at 6w			Prediction of CR at 6m		
	AUC	95% CI	<i>p</i> <sup>a</sup>	AUC	95% CI	<i>pa</i> <sup>a</sup>	AUC	95% CI	<i>pa</i> <sup>a</sup>
Baseline TS	0.742	0.496–0.989	0.108	0.857	0.663–1.000	<i>0.015</i>	0.905	0.561–0.998	0.053
Baseline peritumoural LS	0.655	0.386–0.923	0.336	0.857	0.642–1.000	<i>0.017</i>	0.857	0.505–0.991	0.087
Baseline LS remote from tumour	0.696	0.443–0.950	0.243	0.667	0.387–0.948	0.233	0.917	0.535–0.984	0.096
Baseline serum AFP	0.798	0.591–1.000	<i>0.039</i>	0.798	0.595–1.000	<i>0.025</i>	0.767	0.459–0.948	0.176
Baseline tumour size	0.622	0.295–0.949	0.405	0.631	0.367–0.894	0.342	0.630	0.316–0.878	0.684

<sup>a</sup>Mann-Whitney *U* testItalicised *p* values denote significance

microscopy studies that anti-cancer therapy results in increased tumour cell stiffness [25, 26]. However, at the macroscopic level probed by MRE, characteristic effects of RE such as perivascular oedema, inflammation, necrosis, and extracellular matrix restructuring [10, 27] are likely to affect measured stiffness. We see evidence of this in our results, with peritumoural liver parenchyma also demonstrating increased stiffness following RE. This change is potentially due to the radiation effect on surrounding liver parenchyma by the <sup>90</sup>Y microspheres embedded in the tumour periphery and associated oedema and inflammation. We found no significant change in liver parenchyma stiffness remote to the tumour following RE, which supports this hypothesis.

A cross-sectional study by Gordic et al (16) reported lower TS in HCCs treated with different locoregional treatments (RE, chemoembolisation, radiofrequency ablation) vs untreated HCCs in different populations of patients. Our study has several differences from the study by Gordic et al, such as the acquisition of pre- and post-treatment stiffness data and a shorter interval between treatment and imaging (42 vs 84 days). Another difference is that of the 52 patients who underwent locoregional therapy in the study by Gordic et al, 20/52 received RE and 32 received combined chemoembolisation/radiofrequency ablation. The time course of TS changes following RE is not known. However, it is possible that a reduction in inflammation, interstitial pressure, and perivascular oedema in tumours more than 6w following RE may result in decreasing TS over time.

Baseline TS and peritumoural LS were lower in patients who achieved CR at 6w, i.e. 100% tumour necrosis. The lower baseline TS finding is in agreement with a recent ultrasound elastography study which found that lower baseline HCC stiffness resulted in a better response to chemoembolisation [28]. Another ultrasound elastography study of tumour response to neoadjuvant chemotherapy in breast cancer noted softer tumours showed greater response than stiffer tumours [29]. Basic research studies have shown that tumour

extracellular matrix cross-linking modulates tumour progression in breast cancer cells [30] and elevated stiffness promotes proliferation and resistance to chemotherapy in HCC cells [31]. The finding of lower baseline peritumoural LS in patients who achieved CR at 6w suggests the surrounding liver parenchyma was less fibrotic with potentially lower inflammation than the peritumoural parenchyma in patients who did not achieve CR at 6w. A recent pre-clinical study found that HCCs developed in stiffer livers grew faster and had markedly elevated Ki-67 expression compared to HCCs in less stiff environments [32], which may reduce the efficacy of RE. Additionally, elevated parenchymal stiffness is a sign of advanced fibrosis/liver cirrhosis which can result in increased hepatic vascular resistance. Our results indicate that high TS or peritumoural LS at baseline may indicate lower chances of achieving complete response with RE and prompt consideration of adjuvant systemic therapies such as immune checkpoint inhibitors or tyrosine kinase inhibitors [33, 34]. In addition to reducing unnecessary radiation dose to the patient and potential expense associated with the treatment, an early indication of potential treatment response may ultimately allow more rapid successful treatment by obviating the need to wait for tumour size changes which may take weeks or months to occur following therapy.

We report that baseline serum AFP was a predictor of tumour response at 6w. Serum AFP has been considered a marker of tumour burden; however, several studies have reported poor performance in detecting HCC [35, 36]. The literature contains conflicting evidence regarding the utility of serum AFP in predicting both overall survival and radiological response following RE [37–40]. Further research in a larger cohort is required to confirm our results and determine whether MRE provides an advantage over (or in combination) with serum AFP. A high proportion of HCCs are unresectable; thus, predictive imaging biomarkers of tumour response such as tissue stiffness may provide a clinical benefit by informing treatment strategies and can potentially offer additional

information regarding tumour biology over other measures such as serum AFP.

We found a significant correlation between tumour size and TS at baseline. This is in agreement with other studies which reported a significant [21, 41] or non-significant correlation [15] between tumour size and stiffness. Two other studies noted no significant relationship between tumour size and stiffness; however, in one study, it is not clear if the comparison was performed on untreated HCCs alone [20] and, in the other, non-enhancing or necrotic tumour regions were not included in the MRE ROI (which differs from our methodology) and the mean tumour size was larger than that found in our cohort (5.3 vs 3.2 cm) [18]. HCCs are known to display inter- and intra-tumour heterogeneity [42] and so for larger tumours, stiffness variability may occur owing to heterogeneous tumour components.

In this study, all included tumours were confirmed HCCs and so there was no requirement for classification between malignant and benign tumours. Previous MRE work has shown that tumour viscoelastic properties such as storage modulus, loss modulus, and phase angle (also referred to as damping ratio in the literature) may provide additional benefit over the traditionally reported tumour stiffness (based on the magnitude of the complex shear modulus) [16, 17]. In both previous studies assessing tumour viscoelasticity, 3D MRE methods were applied which is not the case in the current study. In addition, MRE data in the current study were reconstructed using a commercial MRE inversion algorithm which does not provide additional viscoelastic parameter outputs. The change in tumour viscoelastic properties following RE and their utility for prediction of response to RE would be of interest and should be explored in future studies.

Our study has several limitations. The first is the small sample size, with only 23 subjects included in analysis, of which 14 had complete pre- and post-RE data. The second issue is a lack of pathological analysis of the lesions, as it is not common to biopsy tumours once clinical imaging criteria for HCC have been met. The third issue is a lack of MRE after 6w, which would have provided additional information about dynamic changes over time. Further prospective studies are required to inform this. The final issue is, as previously mentioned, the use of 2D MRE for tumour stiffness measurement. In 2D MRE, only the wave propagation in the through-plane axis is encoded into the MR phase image. This method has been shown to provide excellent accuracy in predicting global liver fibrosis measurement [11, 13]; however, in heterogeneous tissues such as a tumour embedded in liver parenchyma, the wave propagation can become disrupted and produce aberrant stiffness measures in tumour and peritumoural parenchyma. 3D MRE captures the wave field in all three orthogonal directions and can address the issue of non-planar wave propagation. The role of 3D MRE in predicting response to therapy should be explored in future studies.

## Conclusion

Our initial results indicate that there are measurable changes in TS and peritumoural LS following RE. Baseline TS, peritumoural LS, and serum AFP appear to be fair/excellent predictors of CR of HCC to RE at 6w. The exact mechanisms and time scales of TS variation following treatment have yet to be fully elucidated and prospective longitudinal studies incorporating pathological correlation with MRE stiffness measurements would be valuable.

**Acknowledgements** The authors thank the participants for their time and are grateful to the MR technologists for assistance with imaging.

**Funding** This study was funded through NCI U01 CA172320.

## Compliance with ethical standards

**Guarantor** The scientific guarantor of this publication is Bachir Taouli.

**Conflict of interest** The other authors of this manuscript declare no relationships with any companies, whose products or services may be related to the subject matter of the article.

**Statistics and biometry** No complex statistical methods were necessary for this paper.

**Informed consent** Written informed consent was obtained from all subjects (patients) in this study.

**Ethical approval** Institutional Review Board approval was obtained.

**Study subjects or cohorts overlap** The patients reported in this study have been reported previously. There is no overlap in MR data between the studies. MR elastography data reported here has not been previously reported.

## Methodology

- prospective
- Observational - longitudinal study
- performed at one institution

## References

1. Kulik LM, Atassi B, van Holsbeeck L et al (2006) Yttrium-90 microspheres (TheraSphere) treatment of unresectable hepatocellular carcinoma: downstaging to resection, RFA and bridge to transplantation. *J Surg Oncol* 94:572–586
2. Lewandowski RJ, Geschwind JF, Liapi E, Salem R (2011) Transcatheter intraarterial therapies: rationale and overview. *Radiology* 259:641–657
3. Semaan S, Makkar J, Lewis S, Chatterji M, Kim E, Taouli B (2017) Imaging of hepatocellular carcinoma response after (90)Y radioembolisation. *AJR Am J Roentgenol* 209:W263–W276
4. Lencioni R, Llovet JM (2010) Modified RECIST (mRECIST) assessment for hepatocellular carcinoma. *Semin Liver Dis* 30:52–60

5. Gordic S, Corcuera-Solano I, Stueck A et al (2017) Evaluation of HCC response to locoregional therapy: validation of MRI-based response criteria versus explant pathology. *J Hepatol* 67:1213–1221
6. Elsayes KM, Hooker JC, Agrons MM et al (2017) 2017 Version of LI-RADS for CT and MR imaging: an update. *Radiographics* 37:1994–2017
7. Deng J, Miller FH, Rhee TK et al (2006) Diffusion-weighted MR imaging for determination of hepatocellular carcinoma response to yttrium-90 radioembolisation. *J Vasc Interv Radiol* 17:1195–1200
8. Gordic S, Wagner M, Zanato R et al (2019) Prediction of hepatocellular carcinoma response to (90)Yttrium radioembolisation using volumetric ADC histogram quantification: preliminary results. *Cancer Imaging* 19:29
9. Barker HE, Paget JT, Khan AA, Harrington KJ (2015) The tumour microenvironment after radiotherapy: mechanisms of resistance and recurrence. *Nat Rev Cancer* 15:409–425
10. Ibrahim SM, Nikolaidis P, Miller FH et al (2009) Radiologic findings following Y90 radioembolisation for primary liver malignancies. *Abdom Imaging* 34:566–581
11. Kennedy P, Wagner M, Castera L et al (2018) Quantitative elastography methods in liver disease: current evidence and future directions. *Radiology* 286:738–763
12. Chang W, Lee JM, Yoon JH et al (2016) Liver fibrosis staging with MR elastography: comparison of diagnostic performance between patients with chronic hepatitis B and those with other etiologic causes. *Radiology* 280:88–97
13. Morisaka H, Motosugi U, Glaser KJ et al (2016) Comparison of diagnostic accuracies of two- and three-dimensional MR elastography of the liver. *J Magn Reson Imaging*. <https://doi.org/10.1002/jmri.25425>
14. Yin M, Glaser KJ, Talwalkar JA, Chen J, Manduca A, Ehman RL (2016) Hepatic MR elastography: clinical performance in a series of 1377 consecutive examinations. *Radiology* 278:114–124
15. Venkatesh SK, Yin M, Glockner JF et al (2008) MR elastography of liver tumors: preliminary results. *AJR Am J Roentgenol* 190:1534–1540
16. Garteiser P, Doblaz S, Daire J-L et al (2012) MR elastography of liver tumours: value of viscoelastic properties for tumour characterisation. *Eur Radiol* 22:2169–2177
17. Shahryari M, Tzschatzsch H, Guo J et al (2019) Tomoelastography distinguishes noninvasively between benign and malignant liver lesions. *Cancer Res* 79:5704–5710
18. Thompson SM, Wang J, Chandan VS et al (2017) MR elastography of hepatocellular carcinoma: correlation of tumor stiffness with histopathology features-preliminary findings. *Magn Reson Imaging* 37:41–45
19. Wang J, Shan Q, Liu Y et al (2019) 3D MR elastography of hepatocellular carcinomas as a potential biomarker for predicting tumor recurrence. *J Magn Reson Imaging* 49:719–730
20. Gordic S, Ayache JB, Kennedy P et al (2017) Value of tumor stiffness measured with MR elastography for assessment of response of hepatocellular carcinoma to locoregional therapy. *Abdom Radiol (NY)*. <https://doi.org/10.1007/s00261-017-1066-y>: 1–10
21. Qayyum A, Hwang KP, Stafford J et al (2019) Immunotherapy response evaluation with magnetic resonance elastography (MRE) in advanced HCC. *J Immunother Cancer* 7:329
22. Silva AM, Grimm RC, Glaser KJ et al (2015) Magnetic resonance elastography: evaluation of new inversion algorithm and quantitative analysis method. *Abdom Imaging* 40:810–817
23. Schneider CA, Rasband WS, Eliceiri KW (2012) NIH Image to ImageJ: 25 years of image analysis. *Nat Methods* 9:671–675
24. Vogl TJ, Martin SS, Johnson AA, Haas Y (2020) Evaluation of MR elastography as a response parameter for transarterial chemoembolisation of colorectal liver metastases. *Eur Radiol*
25. Lam WA, Rosenbluth MJ, Fletcher DA (2007) Chemotherapy exposure increases leukemia cell stiffness. *Blood* 109:3505–3508
26. Raudenska M, Kratochvilova M, Vicar T et al (2019) Cisplatin enhances cell stiffness and decreases invasiveness rate in prostate cancer cells by actin accumulation. *Sci Rep* 9:1660
27. Spina JC, Hume I, Pelaez A, Peralta O, Quadrelli M, Garcia Monaco R (2019) Expected and unexpected imaging findings after (90)Y transarterial radioembolisation for liver tumors. *Radiographics* 39:578–595
28. Chen R, Kong W, Gan Y et al (2019) Tumour stiffness associated with tumour response to conventional transarterial chemoembolisation for hepatocellular carcinoma: preliminary findings. *Clin Radiol* 74:814.e811–814.e817
29. Hayashi M, Yamamoto Y, Ibusuki M et al (2012) Evaluation of tumor stiffness by elastography is predictive for pathologic complete response to neoadjuvant chemotherapy in patients with breast cancer. *Ann Surg Oncol* 19:3042–3049
30. Levental KR, Yu H, Kass L et al (2009) Matrix crosslinking forces tumor progression by enhancing integrin signaling. *Cell* 139:891–906
31. Schrader J, Gordon-Walker TT, Aucott RL et al (2011) Matrix stiffness modulates proliferation, chemotherapeutic response, and dormancy in hepatocellular carcinoma cells. *Hepatology* 53:1192–1205
32. Dong Y, Zheng Q, Wang Z et al (2019) Higher matrix stiffness as an independent initiator triggers epithelial-mesenchymal transition and facilitates HCC metastasis. *J Hematol Oncol* 12:112
33. Finn RS, Qin S, Ikeda M et al (2020) Atezolizumab plus bevacizumab in unresectable hepatocellular carcinoma. *N Engl J Med* 382:1894–1905
34. Lee MS, Ryoo BY, Hsu CH et al (2020) Atezolizumab with or without bevacizumab in unresectable hepatocellular carcinoma (GO30140): an open-label, multicentre, phase 1b study. *Lancet Oncol* 21:808–820
35. Lok AS, Sterling RK, Everhart JE et al (2010) Des- $\gamma$ -carboxy prothrombin and  $\alpha$ -fetoprotein as biomarkers for the early detection of hepatocellular carcinoma. *Gastroenterology* 138:493–502
36. Trevisani F, D'Intino PE, Morselli-Labate AM et al (2001) Serum  $\alpha$ -fetoprotein for diagnosis of hepatocellular carcinoma in patients with chronic liver disease: influence of HBsAg and anti-HCV status. *J Hepatol* 34:570–575
37. Memon K, Kulik L, Lewandowski RJ et al (2012) Alpha-fetoprotein response correlates with EASL response and survival in solitary hepatocellular carcinoma treated with transarterial therapies: a subgroup analysis. *J Hepatol* 56:1112–1120
38. Riaz A, Ryu RK, Kulik LM et al (2009) Alpha-fetoprotein response after locoregional therapy for hepatocellular carcinoma: oncologic marker of radiologic response, progression, and survival. *J Clin Oncol* 27:5734–5742
39. Spreafico C, Sposito C, Vaiani M et al (2018) Development of a prognostic score to predict response to Yttrium-90 radioembolisation for hepatocellular carcinoma with portal vein invasion. *J Hepatol* 68:724–732
40. Bhutiani N, O'Brien SJ, Priddy EE et al (2020) Correlating serum alpha-fetoprotein in hepatocellular carcinoma with response to Yttrium-90 transarterial radioembolisation with glass microspheres (TheraSphere™). HPB (Oxford). <https://doi.org/10.1016/j.hpb.2019.12.007>
41. Hennedige TP, Hallinan JTPD, Leung FP et al (2016) Comparison of magnetic resonance elastography and diffusion-weighted imaging for differentiating benign and malignant liver lesions. *Eur Radiol* 26:398–406
42. Friemel J, Rechsteiner M, Frick L et al (2015) Intratumor heterogeneity in hepatocellular carcinoma. *Clin Cancer Res* 21:1951–1961